

# A Cost-Driven Fuzzy Scheduling Strategy for Intelligent Workflow Decision Making Systems in Uncertain Edge-Cloud Environments

Bing Lin, Chaowei Lin, and Xing Chen, *Member, IEEE*

**Abstract**—Workflow decision making is critical to performing many practical workflow applications. Scheduling in edge-cloud environments can address the high complexity problem of workflow applications, while decreasing the data transmission delay between the cloud and end devices. However, because of the heterogeneous resources in edge-cloud environments and the complicated data dependencies among the tasks in a workflow, significant challenges for workflow scheduling remain, including the selection of an optimal tasks-servers solution from the possible numerous combinations. The existing studies have been mainly done subject to rigorous conditions without fluctuations, ignoring the fact that workflow scheduling is typically present in uncertain environments. In this study, we focus on reducing the execution cost of workflow applications mainly caused by task computation and data transmission, while satisfying the workflow deadline in uncertain edge-cloud environments. The Triangular Fuzzy Numbers (TFNs) are adopted to represent the task processing time and data transferring time. A cost-driven fuzzy scheduling strategy based on an Adaptive Discrete Particle Swarm Optimization (ADPSO) algorithm is proposed, which employs the operators of Genetic Algorithm (GA). This strategy introduces the randomly two-point crossover operator, neighborhood mutation operator, and adaptive multipoint mutation operator of GA to effectively avoid converging on local optima. The experimental results show that our strategy can effectively reduce the workflow execution cost in uncertain edge-cloud environments, compared with other benchmark solutions.

**Index Terms**—Decision-making, Uncertain edge-cloud environments, Workflow applications, Cost-driven scheduling strategy, Deadline constraints

## I. INTRODUCTION

WORKFLOWS are widely exploited for the modeling of complicated applications, such as DNN-based applications [1], [2]. Such a workflow is usually computing-intensive, typically composed of tens of interdependent tasks. Indeed, workflow scheduling is essential as its result could directly

This work is partly supported by the Natural Science Foundation of China under Grant No. 62072108, the Natural Science Foundation of Fujian Province for Distinguished Young Scholar No. 2020J06014, and the University-Industry Cooperation of Fujian Province under Grant No. 2022H6024.

Bing Lin is with the College of Physics and Energy, Fujian Normal University, Fujian Provincial Key Laboratory of Quantum Manipulation and New Energy Materials, Fuzhou, 350117, China, Fujian Provincial Collaborative Innovation Center for Advanced High-Field Superconducting Materials and Engineering, Fuzhou, 350117, China, and School of Computer Science, Peking University, 100871, China. E-mail: WheelLX@163.com.

Chaowei Lin and Xing Chen are with the College of Mathematics and Computer Science, Fuzhou University, Fuzhou, 350118, China, and with Fujian Provincial Key Laboratory of Network Computing and Intelligent Information Processing, Fuzhou, 350118, China. E-mail: cwlin1998@foxmail.com, chenxing@fzu.edu.cn.

affect the performance of workflow applications [3]. Due to the complicated structure of a workflow and the sophisticated data dependencies between the tasks in a workflow, completing workflow scheduling in time can be rather challenging even with the use of a high-performance computing platform.

To tackle the aforementioned challenge, some studies have been focused on workflow scheduling in the cloud computing environment [4]–[6]. Such work is mainly oriented towards cloud service providers (e.g., Amazon EC2, Rackspace, and GoGrid) which provide virtual resources to the end customers [7], [8]. The underlying techniques have been developed in an attempt to rationally schedule the dependent tasks among the virtual resources through the pay-as-you-go method. However, they are generally aimed at reducing the workflow completion time and improving the resource utilization, with far less a focus on optimizing the execution cost of workflow applications. They mostly ignore the performance variation between virtual machines with different configurations. In terms of scheduling workflow in the cloud, it might increase the traffic load of core networks and cause high latency due to massive data transmission between clients and the cloud [9].

Edge computing provides an essential technology to improve performance in workflow scheduling [10]. It enhances the computing ability of a mobile network through deploying the computation and storage resources around the edges of the mobile web, thereby providing the service with high broadband and low delay to the clients. Workflow scheduling in edge-cloud environments not only meets the compute-intensive requirements of workflow applications, but also effectively reduces data transmission delays, while scheduling the data-intensive tasks to the edge and the compute-intensive tasks to the cloud [11]. Nonetheless, the service nodes (namely, the virtual machines in the cloud and the servers in the edge) are generally heterogeneous and their processing capacities can be rather different, as well as the cost-performance in terms of load/energy consumption [12]. To reduce the workflow execution cost while satisfying deadline constraints, significant difficulties remain in rationally scheduling the data-dependent tasks for efficient data transmissions and task executions.

The existing studies on workflow scheduling are mainly carried out subject to certain conditions (e.g., assuming that the performance of the service nodes, bandwidth, and other factors are steady, without fluctuation) [13]–[15]. However, in the practical scheduling processes, the CPUs of the service nodes and bandwidths between them always fluctuate, which may have considerable impact upon workflow scheduling.

Whilst uncertainties in scheduling have been addressed, the relevant work mainly focused on Fuzzy Job Shop Scheduling Problem (FJSSP) [16], [17] or task scheduling for the real-time embedded systems [18].

The above methods have good inspirations for the workflow scheduling in uncertain edge-cloud environments. However, they suffer from the following limitations:

- Due to the uncertain conditions, the task processing time and data transferring time are usually difficult to determine. Hence, existing workflow scheduling strategies can not be directly applied to the uncertain edge-cloud environments.
- Due to the heterogeneity among servers, there is a non-negligible difference in their execution performance. Hence, the existing methods are difficult to select an optimal cost-driven tasks-servers scheduling solution from the numerous servers.
- Existing workflow scheduling strategies mainly considers factors such as the server load balancing and energy consumption, the workflow completion time and execution cost, and less consideration is given to the comprehensive cost optimization of task computing and data transmission within deadline constraints.

To address the above questions, we develop a novel workflow scheduling strategy to reduce the workflow execution cost caused by task computation and data transmission, while satisfying the required deadline constraints in uncertain edge-cloud environments. The major contributions of this work are summarized below:

- To reasonably model workflow scheduling in uncertain edge-cloud environments, Triangular Fuzzy Numbers (TFNs) [19] are adopted to represent the task processing time and data transferring time.
- To reduce the comprehensive cost of task computing and data transmission within deadline constraints, a cost-driven workflow scheduling strategy based on an Adaptive Discrete Particle Swarm Optimization (ADPSO) algorithm employing the operators of Genetic Algorithm (GA) is proposed, which improves the exploration and exploitation of scheduling strategies to obtain a better result.
- The extensive simulation experiments are conducted. The performance results demonstrate that the proposed strategy can achieve the superior performance than other classic methods with respect to commonly adopted benchmark datasets.

The rest of this paper is organized as follows: Section II briefly reviews the related work. Section III presents the problem of workflow scheduling in uncertain edge-cloud environments. Section IV describes our proposed workflow scheduling strategy in detail. Section V analyzes the performance of our strategy through experimental studies in comparison with the state-of-the-art scheduling strategies. Finally, Section VI summarizes the work and outlines relevant future research directions.

## II. RELATED WORK

A workflow model, used to simulate and analyze the workflow applications in the real world, consists of a set of the computational tasks linked through control and data dependencies [20]. Workflow scheduling is essential as its result could directly affect the performance of workflow applications.

Many research efforts have been launched to workflow scheduling in cloud computing. Yuan *et al.* [4] considered the cost minimization of data centers in private cloud. They proposed a Temporary Task Scheduling Algorithm (TTSA) that could efficiently schedule all arriving tasks to the private or public clouds. This method effectively reduces the cost of the private cloud while satisfying all tasks' delay constraints. Meng *et al.* [6] proposed a security-aware scheduling method based on the PSO algorithm for real-time resource allocation across heterogeneous clouds. Experimental results showed that this strategy could achieve a good balance between scheduling and security performance. Pham *et al.* [21] considered the fulfilment and interruption rates of the volatile resources in order to reflect the instability of the cloud infrastructure. In that work, a novel evolutionary multi-objective workflow scheduling approach was proposed for generating a set of trade-off solutions, whose makespan and cost were superior to the state-of-the-art algorithms. Paknejad *et al.* [22] proposed an enhanced multi-objective co-evolutionary algorithm, called ch-PICEA-g, for workflow scheduling in cloud environment. Experiments results indicated that the proposed algorithm outperformed its counterparts in terms of different performance metrics, such as cost, makespan, and energy consumption. It is of practical significance for scheduling workflow in cloud computing. However, it might increase the traffic load of core networks and cause high latency due to massive data transmission between clients and the cloud.

Edge computing can effectively reduce the system delay of workflow scheduling [10], [11], [23]. Workflow scheduling in edge-cloud environments has recently drawn great interest. For instance, Xie *et al.* [24] designed a novel Directional and Non-local-Convergent PSO (DNCPSO) algorithm to simultaneously optimize the completion time and execution cost of the workflow. Experimental results demonstrated that DNCPSO could achieve better performance than other classic algorithms. Peng *et al.* [25] proposed a node reliability model to evaluate resource reliability in Mobile Edge Computing (MEC) environments, defining workflow scheduling as an optimization problem and solving it by an algorithm based on Krill-Herd [26]. Through experiments based on real workflow applications and mobile user contract tracking, it had proven that the performance of this method was significantly better than the traditional methods in terms of success rate and makespan. However, existing research on workflow scheduling in edge-cloud environments hardly considers the comprehensive cost optimization for task computation and data transmission.

In real-world practice, the performance of service nodes and the bandwidth may fluctuate while scheduling a workflow application. Initial work exists and deals with scheduling in uncertain computing environments, but such work is mainly oriented towards intelligent manufacturing systems. In partic-

ular, Lei [27] represented the fuzzy processing time and fuzzy due-date with TFNs and trapezoidal fuzzy numbers, respectively, while introducing an improved fuzzy max operation to investigate the FJSSP. In that work, so-called availability constraints are employed for maximizing the satisfaction level of customers. Sun *et al* [16] also used TFNs to describe the processing time to cope with the FJSSP problem, where an effective hybrid Cooperative Evolution Algorithm (hCEA) was proposed for minimizing the fuzzy makespan. Fortemps [28] expressed an uncertain duration as a six-point fuzzy number, thereby establishing a fuzzy scheduling model to minimize the fuzzy completion time for job shop scheduling problem. Similarly, Li *et al* [29] used TFNs to capture the uncertainty of fuzzy processing time and introduced a uniform parallel machine scheduling with such processing time representation under fuzzy resource consumption constraints, minimizing the makespan.

Despite the aforementioned remarkable developments in the relevant research area, an important open issue remains on fuzzy workflow scheduling that is of great practical significance: Workflow scheduling that considers the fuzzy task processing time and fuzzy data transferring time in uncertain edge-cloud environments. Inspired by this observation, the remainder of this paper will establish a novel approach to cost-driven scheduling for deadline-based workflows in uncertain edge-cloud environments.

### III. SYSTEM MODEL AND DEFINITIONS

In this section, the workflow scheduling in certain environments is described firstly. Then we further elaborate the workflow scheduling in uncertain environments. Thirdly, the operations for TFNs in fuzzy workflow scheduling are introduced in detail. Finally, an example of cost-driven scheduling for a deadline-based workflow application in uncertain edge-cloud environments is illustrated.

#### A. Workflow Scheduling in Certain Environments

The workflow scheduling framework proposed in this study consists of three main components, *i.e.*, the edge-cloud environments, a deadline-based workflow, and a cost-driven scheduler.

A certain environment means that there is no fluctuation during workflow scheduling and execution. The edge-cloud environments  $\mathcal{S} = \{\mathcal{S}_{cloud}, \mathcal{S}_{edge}\}$  consist of the cloud and edge, where there are different computing nodes (*i.e.*, virtual machines in the cloud and servers in the edge). For simplicity, we use ‘servers’ to denote the computing nodes in the cloud and edge with a uniform representation. There are  $n$  servers in the cloud  $\mathcal{S}_{cloud} = \{s_1, s_2, \dots, s_n\}$ , and  $m$  servers in the edge  $\mathcal{S}_{edge} = \{s_{n+1}, s_{n+2}, \dots, s_{n+m}\}$ . A server  $s_i$  is denoted by Eq. (1).

$$s_i = (\zeta_i, \varpi_i, p_i, c_i^{com}, \lambda_i, f_i), \quad (1)$$

where  $\zeta_i$  and  $\varpi_i$  are the booting time and shutdown time of the server  $s_i$ , respectively;  $p_i$  is the processing capacity of the server  $s_i$ ;  $c_i^{com}$  is the computation cost per time unit  $\lambda_i$ ,

which is a specific time unit for the server  $s_i$ ;  $f_i = \{0, 1\}$  refers to the platform to which the server  $s_i$  belongs. Note that when  $f_i = 0$ ,  $s_i$  belongs to the cloud with powerful processing capacity. Otherwise,  $s_i$  belongs to the edge with normal processing capacity.

The bandwidth  $b_{i,j}$  between any two different servers is denoted by Eq. (2).

$$b_{i,j} = (\beta_{i,j}, c_{i,j}^{tran}), \quad (2)$$

where  $\beta_{i,j}$  is the value of the bandwidth  $b_{i,j}$ ,  $\forall i, j = 1, 2, \dots, |\mathcal{S}|, i \neq j$ ;  $c_{i,j}^{tran}$  is the data transmission cost per GB from the server  $s_i$  to  $s_j$ .

A workflow can be described as a directed acyclic graph (DAG)  $\mathbf{W} = (\mathbf{V}, \mathbf{E})$ , where  $\mathbf{V} = \{v_1, v_2, \dots, v_l\}$  is a finite set of  $l$  tasks, and  $\mathbf{E} = \{e_{i,j} = \langle v_i, v_j \rangle | v_i, v_j \in \mathbf{V}, \forall i \neq j\}$  is a finite set of directed arcs. Each directed arc  $e_{i,j} = \langle v_i, v_j \rangle$  indicates that there is a dataset  $d_{i,j}$  transferred from the task  $v_i$  to  $v_j$ , and  $v_j$  cannot be executed until  $v_i$  is finished. For an arc  $e_{i,j} = \langle v_i, v_j \rangle$ ,  $v_i$  is called the immediate predecessor task of  $v_j$ , and  $v_j$  is called the immediate successor task of  $v_i$ . In addition, a workflow has a corresponding deadline constraint  $D(\mathbf{W})$ . When a workflow is completed within its deadline based on a specific scheduling strategy, this strategy is called as a feasible solution.

Suppose that the processing time of the task  $v_i$  on the server  $s_j$  is described as  $t_{com}(v_i, s_j)$ . Owing to its popularity, the serial processing model [30] is adopted herein. It expresses that a task is processed on only one server, and a server can process only one task concurrently. The data transferring time  $t_{tran}(d_{i,j}, s_k, s_l)$  is denoted by Eq. (3).

$$t_{tran}(d_{i,j}, s_k, s_l) = \frac{d_{i,j}}{\beta_{k,l}}, \quad (3)$$

where  $t_{tran}(d_{i,j}, s_k, s_l)$  is the time to transfer the dataset  $d_{i,j}$  from the server  $s_k$  to  $s_l$ . If  $s_k$  and  $s_l$  are the same server, the data transferring time is 0.

A cost-driven scheduler aims to reduce the workflow execution cost mainly caused by task computation and data transmission, while satisfying its deadline in edge-cloud environments. A scheduling strategy  $\Psi$  is denoted by Eq. (4).

$$\Psi = (\mathbf{W}, \mathcal{S}, \mathbf{M}, t_t, c_t), \quad (4)$$

where  $\mathbf{M} = \{(v_i, s_j) \cup (d_{k,l}, s_r, s_t) | v_i \in \mathbf{V}, d_{k,l} \in \mathbf{E}, s_j, s_r, s_t \in \mathcal{S}\}$  is the mapping from the tasks and datasets to the servers;  $t_t$  is the workflow completion time, and  $c_t$  is the workflow execution cost in edge-cloud environments with a given scheduling strategy.

There are two subsets in the mapping  $\mathbf{M}$ :  $(v_i, s_j)$  indicates that the task  $v_i$  is executed on the server  $s_j$ , and  $(d_{k,l}, s_r, s_t)$  implies that the dataset  $d_{k,l}$  is transferred from the server  $s_r$  to  $s_t$ . When the subset  $\mathbf{M}_{\mathbf{V}} = \{(v_i, s_j) | v_i \in \mathbf{V}, s_j \in \mathcal{S}\}$  is determined, the other subset  $\mathbf{M}_{\mathbf{E}} = \{(d_{k,l}, s_r, s_t) | d_{k,l} \in \mathbf{E}, s_r, s_t \in \mathcal{S}\}$  will be determined. Therefore, the mapping  $\mathbf{M}$  is equivalent to  $\mathbf{M}_{\mathbf{V}}$  as Eq. (5).

$$\mathbf{M} = \mathbf{M}_{\mathbf{V}} = \{(v_i, s_j) | v_i \in \mathbf{V}, s_j \in \mathcal{S}\}. \quad (5)$$

When the mapping  $M$  is determined, the servers processing all tasks are determined with a specific scheduling strategy  $\Psi$ . Due to the data dependencies between the tasks in a workflow, the execution order of each task is relatively fixed. Each task  $v_i$  will have the start time  $t_{start}(v_i)$  and the end time  $t_{end}(v_i)$  once the corresponding  $M$  is determined. The workflow completion time can be denoted by Eq. (6).

$$t_t = \max_{v_i \in \mathbf{V}} \{t_{end}(v_i)\}. \quad (6)$$

We assume that the shutdown time  $\varpi_i$  of  $s_i$  is equal to the end time of the last task on it. The total execution cost  $c_t$  of scheduling a workflow in edge-cloud environments is determined by Eqs. (7-9).

$$c_t = c_{com} + c_{tran}, \quad (7)$$

$$c_{com} = \sum_{i=1}^{|\mathbf{S}|} c_i^{com} \cdot \left\lfloor \frac{\varpi_i - \zeta_i}{\lambda_i} \right\rfloor, \quad (8)$$

$$c_{tran} = \sum_{v_j \in \mathbf{V}} \sum_{v_k \in \mathbf{V}} c_{r,t}^{tran} \cdot d_{j,k}(v_j, s_r), (v_k, s_t) \in \mathbf{M}, \quad (9)$$

where  $c_{com}$  is the task computation cost, and  $c_{tran}$  is the data transmission cost.

In summary, the scheduling strategy for a workflow in certain environments can be described by Eq. (10), which indicates that the scheduler pursues to minimize the total workflow execution cost  $c_t$ , while satisfying its deadline  $D(\mathbf{W})$ .

$$\begin{cases} \min c_t; \\ s.t. t_t \leq D(\mathbf{W}). \end{cases} \quad (10)$$

### B. Workflow Scheduling in Uncertain Environments

Uncertain environments mean that there are fluctuations during workflow scheduling and execution. The task processing time and data transferring time are uncertain due to the fluctuations of server processing capacity and bandwidth, respectively. Fuzzy set are employed to reflect the uncertainties during workflow execution, while the task processing time and data transferring time are represented as TFNs.

The membership function  $\mu_{\tilde{t}}(x)$  of a TFN  $\tilde{t} = (t^l, t^m, t^u)$  can be denoted by Eq. (11), which is represented graphically as Fig. 1 [31].

$$\mu_{\tilde{t}}(x) = \begin{cases} \frac{x-t^l}{t^m-t^l}, & x \in [t^l, t^m]; \\ \frac{x-t^u}{t^m-t^u}, & x \in [t^m, t^u]; \\ 0, & x \in (-\infty, t^l) \cup (t^u, +\infty). \end{cases} \quad (11)$$

Where  $t^m$  is the normal (namely, the most possible) value of the fuzzy variable  $\tilde{t}$ ;  $t^l$  and  $t^u$  are the lower and upper limit values of  $\tilde{t}$ , respectively. When  $t^l = t^m = t^u$ ,  $\tilde{t}$  is a certain number. A fuzzy variable  $\tilde{\tau}$  in uncertain environments corresponds to a variable  $\tau$  in certain environments. According to the principles of fuzzy set theory [32], the scheduling strategy for a workflow in uncertain environments can be defined as Eq. (12).

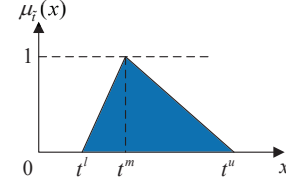


Fig. 1. The membership function  $\mu_{\tilde{t}}(x)$  of a TFN  $\tilde{t}$

$$\begin{cases} \min \tilde{c}_t; \\ s.t. \tilde{t}_t \leq D(\mathbf{W}). \end{cases} \quad (12)$$

Where  $\tilde{c}_t$  is the fuzzy total workflow execution cost, and  $\tilde{t}_t$  is the fuzzy workflow completion time. Both fuzzy variables (i.e.,  $\tilde{c}_t$  and  $\tilde{t}_t$ ) are represented by TFNs. For the target  $\min \tilde{c}_t$ , an equivalent representation through its mean value and the standard deviation can be introduced [33], where the objective function given in Eq. (12) is equivalent to that Eq. (13).

$$\begin{aligned} \min \tilde{c}_t &= (c^l, c^m, c^u) \Rightarrow \\ \min m(\tilde{c}_t) + \eta \cdot std(\tilde{c}_t), \eta &\geq 0. \end{aligned} \quad (13)$$

Where  $m(\tilde{c}_t)$  and  $std(\tilde{c}_t)$  are the mean value and standard deviation of  $\tilde{c}_t$ , and  $\eta$  is the weighting factor of  $std(\tilde{c}_t)$ . According to the work of Lee and Li [33], the mean value and standard deviation of a TFN can be defined through uniform distribution and proportional distribution. Therefore,  $m(\tilde{c}_t)$  and  $std(\tilde{c}_t)$  can be computed as Eqs. (14) and (15), respectively.

$$m(\tilde{c}_t) = \frac{\int x \tilde{c}_t^2(x) dx}{\int \tilde{c}_t^2(x) dx} = \frac{c^l + 2c^m + c^u}{4}, \quad (14)$$

$$\begin{aligned} std(\tilde{c}_t) &= \left[ \frac{\int x^2 \tilde{c}_t^2(x) dx}{\int \tilde{c}_t^2(x) dx} - m^2(\tilde{c}_t) \right]^{1/2} \\ &= \left[ \frac{2(c^l - c^m)^2 + (c^l - c^u)^2 + 2(c^m - c^u)^2}{80} \right]^{1/2}. \end{aligned} \quad (15)$$

In the process of workflow scheduling, the actual task processing time and data transferring time are more likely to be longer than the estimated values [34]. A new fuzzification method based on Sun *et al.* [16] is proposed to describe the uncertain values (namely, the task processing time and data transferring time). Therefore, the related parameters of a TFN  $\tilde{t} = (t^l, t^m, t^u)$  are redefined as follows:  $t^m$  is the estimated time;  $t^l$  and  $t^u$  are randomly selected from the interval  $[\delta_1 \cdot t, t]$  and  $[2t - t^l, \delta_2 \cdot t]$ , respectively, where  $\delta_1 < 1$ ,  $\delta_2 > 1$  and  $\delta_2 - 1 > 1 - \delta_1$ .

Such a TFN will satisfy the constraint  $t^u - t^m \geq t^m - t^l$ . Therefore, the mean value  $m(\tilde{t})$  of a TFN  $\tilde{t}$  becomes that in Eq. (16), which is more likely to be longer than its estimate.

$$m(\tilde{t}) = \frac{t^l + 2t^m + t^u}{4} \geq t^m = t. \quad (16)$$

For the constraint  $\tilde{t}_t \leq D(\mathbf{W})$ , the upper limit value  $t^u$  of  $\tilde{t}_t$  should be no more than the deadline constraint in the worst

case. Therefore, the constraint given in Eq. (12) is equivalent to that in Eq. (17).

$$\tilde{t}_t = (t^l, t^m, t^u) \leq D(\mathbf{W}) \Rightarrow t^u \leq D(\mathbf{W}). \quad (17)$$

In summary, the scheduling strategy for a workflow in uncertain edge-cloud environments can be formalized as Eq. (18).

$$\begin{cases} \min & m(\tilde{c}_t) + \eta \cdot \text{std}(\tilde{c}_t); \\ \text{s.t.} & t^u \leq D(\mathbf{W}). \end{cases} \quad (18)$$

### C. Operations for TFNs in Fuzzy Workflow Scheduling

To construct a feasible schedule for a workflow in uncertain edge-cloud environments, the operations for TFNs (*i.e.*, addition, ranking, max, and multiplication) need to be introduced as follows:

1) *Addition Operation*: Addition operation is used to calculate the end time of tasks. Suppose that the start time and processing time of a task are denoted by  $\tilde{r} = (r^l, r^m, r^u)$  and  $\tilde{t} = (t^l, t^m, t^u)$ , respectively. The end time of such a task  $\tilde{e} = (e^l, e^m, e^u)$  is calculated by Eq. (19) [31].

$$\tilde{e} = \tilde{r} + \tilde{t} = (r^l + t^l, r^m + t^m, r^u + t^u). \quad (19)$$

2) *Ranking Operation*: Ranking operation is required to calculate the maximum end time of all the immediate predecessors of the task  $v_i$ . Suppose that the end time of one predecessor and that of another predecessor are  $\tilde{r} = (r^l, r^m, r^u)$  and  $\tilde{t} = (t^l, t^m, t^u)$ , respectively. The maximum end time of such two predecessors is then calculated with respect to three different situations, following the ranking criterion proposed by Sakawa *et al.* [35].

- If  $\alpha_1(\tilde{r}) = (r^l + 2r^m + r^u)/4 > \alpha_1(\tilde{t}) = (t^l + 2t^m + t^u)/4$ , then  $\tilde{r} > \tilde{t}$ .
- If  $\alpha_1(\tilde{r}) = \alpha_1(\tilde{t})$  and  $\alpha_2(\tilde{r}) = r^m > \alpha_2(\tilde{t}) = t^m$ , then  $\tilde{r} > \tilde{t}$ .
- If  $\alpha_1(\tilde{r}) = \alpha_1(\tilde{t})$ ,  $\alpha_2(\tilde{r}) = \alpha_3(\tilde{t})$  and  $\alpha_3(\tilde{r}) = r^u - r^l > \alpha_3(\tilde{t}) = t^u - t^l$ , then  $\tilde{r} > \tilde{t}$ .

Note that multiple ranking operations are recursively performed if there are more than two predecessor tasks.

3) *Max Operation*: Max operation is needed to calculate the start time of tasks. Suppose that the maximum end time of all immediate predecessors of the task  $v_i$  is  $\tilde{r} = (r^l, r^m, r^u)$ , and the last idle time of a server before processing the task  $v_i$  is  $\tilde{t} = (t^l, t^m, t^u)$ . Then, the membership function  $\mu_{\tilde{e}}(z)$  of  $v_i$ 's start time  $\tilde{e} = \tilde{r} \vee \tilde{t}$  is computed by Eq. (20).

$$\begin{aligned} \mu_{\tilde{e}}(z) &= \mu_{\tilde{r} \vee \tilde{t}}(z) = \sup_{z=x \vee y} \min(\mu_{\tilde{r}}(x), \mu_{\tilde{t}}(y)) \\ &\triangleq \bigvee_{z=x \vee y} (\mu_{\tilde{r}}(x) \wedge \mu_{\tilde{t}}(y)). \end{aligned} \quad (20)$$

According to the max criterion proposed by Lei [27], the start time of the task  $v_i$  can be approximated by Eq. (21).

$$\tilde{e} = \tilde{r} \vee \tilde{t} \cong \begin{cases} \tilde{r}, & \tilde{r} \geq \tilde{t}; \\ \tilde{t}, & \tilde{r} < \tilde{t}. \end{cases} \quad (21)$$

TABLE I  
BANDWIDTHS BETWEEN DIFFERENT SERVERS

$f_i$	$\leftrightarrow$	$f_j$	$\beta_{i,j}(\text{MB}\cdot\text{s}^{-1})$	$c_{i,j}^{\text{tran}}(\$. \text{GB}^{-1})$
0	$\leftrightarrow$	0	2.5	0.4
0	$\leftrightarrow$	1	1.0	0.16
1	$\leftrightarrow$	1	12.5	0.8

4) *Multiplication Operation*: Multiplication operation is carried out to calculate the task computation cost and data transmission cost as addressed by Eqs. (8) and (9), respectively. The product of a TFN  $\tilde{t} = (t^l, t^m, t^u)$  and a real number  $\kappa$  is computed by Eq. (22) [31].

$$\kappa \cdot \tilde{t} = (\kappa \cdot t^l, \kappa \cdot t^m, \kappa \cdot t^u), \forall \kappa \in \mathbb{R}. \quad (22)$$

Similarly, the quotient of a TFN  $\tilde{t} = (t^l, t^m, t^u)$  divided by a real number  $v$  can be transformed into the product of such a TFN and another real number as Eq. (23).

$$\tilde{t} \div v \triangleq \kappa \cdot \tilde{t}, \kappa = 1/v, \forall v \in \mathbb{R}. \quad (23)$$

### D. Illustration of Cost-Driven Workflow Scheduling

Fig. 2 presents an example of cost-driven scheduling for a deadline-based workflow in uncertain edge-cloud environments. The edge-cloud environments  $\mathcal{S} = \{s_1, s_2, s_3, s_4\}$  consist of four servers, where  $s_1, s_2$  belong to the cloud and  $s_3, s_4$  belong to the edge. The workflow application has 8 tasks and 9 datasets, whose deadline is  $7.2 \times 10^3 \text{s}$ . The time unit  $\lambda_i$  is set to  $60 \text{s}$ . Table I lists the relevant parameters for the bandwidths between different servers. Table II presents the computation cost per hour for all servers. Table III shows the fuzzy processing time for each task on the available servers.

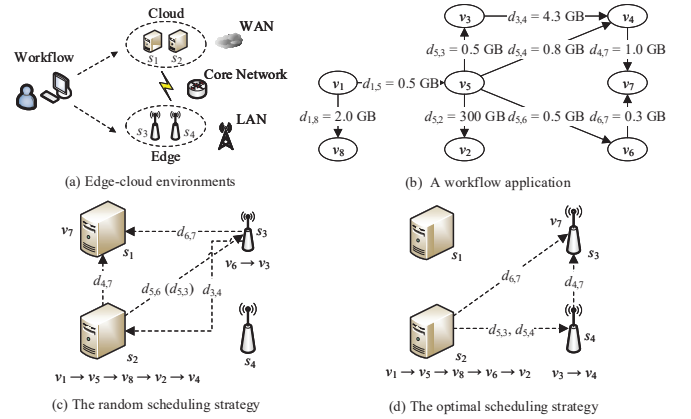


Fig. 2. An example of cost-driven scheduling for a deadline-based workflow application in uncertain edge-cloud environments.

Fig. 2(c) depicts the workflow scheduling results based on the random scheduling strategy [36]. It randomly schedules each task to their corresponding servers, and all tasks are executed according to their data dependencies. The fuzzy completion time  $\tilde{t}_t$  of the workflow application is  $(11599.95 \text{s}, 11599.96 \text{s}, 11613.64 \text{s})$ , which exceeds the corresponding deadline (*i.e.*,  $7.2 \times 10^3 \text{s}$ ). The fuzzy execution cost  $\tilde{c}_t$  based

TABLE II  
COMPUTATION COST PER HOUR OF ALL SERVERS

Servers	$c_i^{com} (\$.h^{-1})$
$s_1$	3.5
$s_2$	13.5
$s_3$	1.5
$s_4$	2.0

on the random scheduling strategy is (38.61\$, 38.84\$, 39.6\$), whose equivalent defuzzified value is 39.14\$. Fig. 2(d) depicts the optimal workflow scheduling. The fuzzy completion time  $\tilde{t}_t$  is (7036.56s, 7052.69s, 7129.24s), which meets its deadline constraint. The fuzzy execution cost  $\tilde{c}_t$  is (28.41\$, 29.84\$, 32.79\$), whose equivalent defuzzified value is 30.93\$. The optimal execution cost is significantly reduced by 21% compared to that based on the random scheduling strategy.

#### IV. OUR PROPOSED INTELLIGENT DECISION MAKING SYSTEMS

The goal of a workflow scheduling strategy,  $\Psi = (\mathbf{W}, \mathbf{S}, \mathbf{M}, \tilde{t}_t, \tilde{c}_t)$ , is to find the best mapping  $\mathbf{M}$  from all tasks in a workflow  $\mathbf{W}$  to different servers in edge-cloud environments  $\mathbf{S}$ , where the workflow execution cost  $\tilde{c}_t$  is optimal within its corresponding deadline  $\tilde{t}_t$ . The tasks on a server have their strict execution order based on the data dependencies. A task can be executed on different servers, and a server also can process many tasks. Therefore, finding the best mapping from all tasks to different servers is a NP-hard problem [37]. PSO is one of the effective algorithms to address such problems. Therefore, we propose a workflow scheduling strategy based on the modified PSO algorithm (*i.e.*, ADPSO). The traditional PSO algorithm is introduced first, followed by a detailed description of ADPSO.

##### A. Traditional PSO Algorithm

PSO is an efficient evolutionary technique inspired by the social behavior of bird flocks. Kennedy and Eberhart first presented the PSO algorithm in 1995 [38], which has been broadly investigated and utilized ever since. The particle is the most significant concept in PSO, which usually represents a candidate solution for an optimization problem. Each particle  $Q_i^t = (X_i^t, V_i^t)$  in a population at the  $t^{\text{th}}$  iteration has its own position  $X_i^t = (x_{i1}^t, x_{i2}^t, \dots, x_{iy}^t)$  and velocity  $V_i^t = (v_{i1}^t, v_{i2}^t, \dots, v_{iz}^t)$ , which will determine their direction and magnitude at the next iteration. The velocity of each particle is affected by their personal best particle  $pB_i^t$  and the global best particle  $gB^t$ . Each particle constantly updates their own velocity and position in the potential solution space to obtain better fitness. The iterative update of velocities and positions for each particle are determined by Eqs. (24) and (25), respectively.

$$V_i^{t+1} = w \cdot V_i^t + c_1 r_1 (pB_i^t - X_i^t) + c_2 r_2 (gB^t - X_i^t), \quad (24)$$

$$X_i^{t+1} = X_i^t + V_i^{t+1}, \quad (25)$$

where  $w$  is an inertia weight, which determines to what extent the velocity of the current particles will affect the corresponding particles of the next generation, having a great impact on the convergence of PSO;  $c_1$  and  $c_2$  are acceleration coefficients, which denote the cognitive ability of a particle for its personal and global best particle, respectively;  $r_1$  and  $r_2$  are the random numbers on the interval [0,1), used to enhance the searching ability of PSO.

The traditional PSO algorithm is designed for continuous optimization problems. However, workflow scheduling in edge-cloud environments is a discrete optimization problem. Therefore, an applicable PSO-based algorithm with new problem encoding and population update needs to be further adjusted.

##### B. ADPSO

The proposed ADPSO are described from five aspects: problem encoding, fitness function, population update, mapping from a particle to a fuzzy scheduling, and parameter settings.

1) *Problem encoding*: Problem encoding affects the searchability of a PSO-based algorithm, which is expected to meet three major principles: *Viability*, *Completeness*, and *Non-redundancy* [39]. Inspired by the work in [40], an order-server nesting strategy is developed to encode the cost-driven workflow scheduling in uncertain edge-cloud environments. In particular, the  $i^{\text{th}}$  particle in the  $t^{\text{th}}$  iteration (*i.e.*,  $P_i^t$ ) is denoted by Eq. (26).

$$P_i^t = \left( (\chi_{i1}, s_{i1})^t, (\chi_{i2}, s_{i2})^t, \dots, (\chi_{i|\mathbf{V}|}, s_{i|\mathbf{V}|})^t \right), \quad (26)$$

where  $(\chi_{ij}, s_{ij})^t, j = 1, 2, \dots, |\mathbf{V}|$ , indicates the assignment of the task  $v_j$ , meaning that  $v_j$  is executed on the server  $s_{ij}$  with a specified order  $\chi_{ij}$ . There are two criteria for the task execution on a server as follows:

**Criterion 1:** If two concurrent tasks without data dependencies (*i.e.*, there are no direct or indirect data dependencies between the tasks) are scheduled to the same server, the task with a larger order value will be processed earlier. If two tasks have the same order value, the one entering pending queue earlier will be processed first.

**Criterion 2:** If two tasks with data dependencies are scheduled to the same server, the predecessor one is processed first.

Task	1	2	3	4	5	6	7	8
Particle	2.3; 2	1.2; 2	0.7; 4	0.9; 4	3.9; 2	1.5; 2	2.3; 3	1.5; 2

Fig. 3. A encoded particle corresponding to the scheduling result of Fig. 2(d).

Fig. 3 depicts an encoded particle corresponding to the scheduling result of Fig. 2(d). After the task  $v_1$  is executed, the tasks  $v_5$  and  $v_8$  are both scheduled to the server  $s_2$ . Since there are no data dependencies between  $v_5$  and  $v_8$ , and  $v_5$  has a larger order value (*i.e.*, 3.9), it is processed first based on **Criterion 1**. The tasks  $v_2, v_3$  and  $v_6$  are next scheduled to the corresponding servers. At this moment,  $v_8, v_2$  and  $v_6$  are in the pending queue of the server  $s_2$ . Whilst  $v_8$  has the same order

TABLE III  
FUZZY PROCESSING TIME FOR EACH TASK ON AVAILABLE SERVERS (UNIT: s)

	$s_1$	$s_2$	$s_3$	$s_4$
$v_1$	(2560.97, 2800, 3484.58)	(618.57, 700, 884.27)	(3406.72, 3500, 3828.08)	(4812.15, 5250, 5974.03)
$v_2$	(13918.81, 14000, 17808.50)	(3323.98, 3500, 3835.46)	(16819.00, 17500, 20539.04)	(25343.82, 26250, 28794.55)
$v_3$	(1144.78, 1200, 1450.83)	(298.19, 300, 303.49)	(1323.77, 1500, 1683.88)	(2089.08, 2250, 2479.93)
$v_4$	(701.05, 800, 1015.21)	(176.64, 200, 258.50)	(973.31, 1000, 1174.42)	(1427.83, 1500, 1936.48)
$v_5$	(1717.10, 2000, 2297.11)	(482.74, 500, 590.05)	(2468.10, 2500, 2889.79)	(3211.60, 3750, 4865.82)
$v_6$	(210.18, 240, 274.81)	(51.30, 60, 77.00)	(283.40, 300, 375.52)	(403.55, 450, 568.21)
$v_7$	(399.99, 400, 413.68)	(96.64, 100, 107.72)	(483.87, 500, 576.55)	(689.23, 750, 881.02)
$v_8$	(7849.11, 8000, 10081.39)	(1817.86, 2000, 2204.68)	(9113.32, 10000, 12923.71)	(14511.28, 15000, 16312.29)

value (*i.e.*, 1.5) as  $v_6$ , it will be processed before  $v_6$  because it enters the pending queue of  $s_2$  earlier. The remaining tasks are similarly processed based on the two criteria.

2) *Fitness function*: Fitness function is used to evaluate the performance of particles. In general, a particle with a small fitness value represents a better candidate solution. This study aims to minimize the fuzzy total execution cost  $\tilde{c}_t$  of scheduling a workflow within its deadline  $D(\mathbf{W})$ . Therefore, a particle corresponding to a scheduling result with a smaller fuzzy execution cost  $\tilde{c}_t$  can be regarded as a better solution. However, the problem encoding strategy may not meet the *Viability* principle, which dictates that the fuzzy completion time  $\tilde{t}_t$  of a workflow must not exceed its deadline  $D(\mathbf{W})$ . Therefore, we compare the performance of two particles following three different situations.

**Situation 1:** Both particles corresponding to the scheduling results are feasible. The one with a smaller fuzzy total execution cost  $\tilde{c}_t$  is deemed better, and the fitness function is defined by Eq. (27).

$$F(P_i) = \tilde{c}_t(P_i) \Rightarrow m(\tilde{c}_t(P_i)) + \eta \cdot std(\tilde{c}_t(P_i)). \quad (27)$$

**Situation 2:** One particle corresponding to the scheduling result is feasible, and the other is infeasible. The feasible particle is naturally deemed better, and the fitness function is defined by Eq. (28).

$$F(P_i^t) = \begin{cases} \tilde{c}_t(P_i^t), \tilde{t}_t(P_i^t) \leq D(w) \\ \infty, \tilde{t}_t(P_i^t) > D(w) \end{cases}$$

$$\Rightarrow \begin{cases} m(\tilde{c}_t(P_i^t)) + \eta \cdot std(\tilde{c}_t(P_i^t)), t^u(P_i^t) \leq D(w); \\ \infty, t^u(P_i^t) > D(w). \end{cases} \quad (28)$$

**Situation 3:** Both particles corresponding to the scheduling results are infeasible. The one with less fuzzy completion time  $\tilde{t}_t$  is deemed better, which is more likely to become feasible after update operations. The fitness function is defined by Eq. (29).

$$F(P_i) = \tilde{t}_t(P_i) \Rightarrow t^u(P_i). \quad (29)$$

3) *Population update*: The update of each particle is affected by three factors: *inertia*, *individual cognition*, and *social cognition* [41]. To strengthen the searchability and avoid

premature convergence of the proposed scheduling strategy, ADPSO employs the mutation operator and crossover operator of GA. The iterative update of the  $i^{\text{th}}$  particle at the  $(t+1)^{\text{th}}$  iteration for the workflow scheduling is defined as Eq. (30).

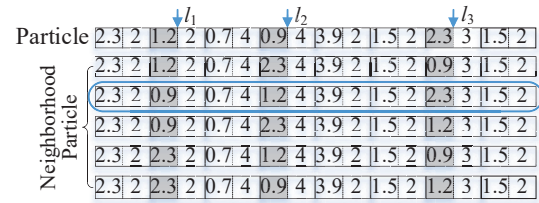
$$P_i^{t+1} = op^{cr}(op^{cr}(op^{mu}(P_i^t, w, r), pB_i^t, c_1, r_1), gB^t, c_2, r_2), \quad (30)$$

where  $op^{mu}()$  and  $op^{cr}()$  are mutation operation and crossover operation, respectively;  $w$  is an inertia weight;  $c_1$  and  $c_2$  are acceleration coefficients;  $r$ ,  $r_1$  and  $r_2$  are random numbers generated from the interval  $[0, 1)$ .

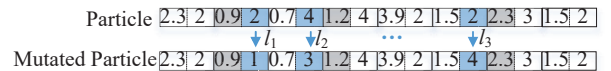
For the *inertia* part, the mutation operator of GA [42] is introduced to perform the updating as Eq. (31).

$$A_i^{t+1} = op^{mu}(P_i^t, w, r) = \begin{cases} M_u(P_i^t), r < w; \\ P_i^t, \text{otherwise.} \end{cases} \quad (31)$$

Where  $M_u()$  denotes the dual mutation operator, which includes the neighborhood mutation operator for the task order and the adaptive multi-point mutation operator for the number of servers.



(a) Neighborhood mutation operator for the task order



(b) Adaptive multi-point mutation operator for number of servers

Fig. 4. Dual mutation operator.

The neighborhood mutation operator randomly chooses three locations in a particle, and generates all sort combinations for the task order in the corresponding field. Then, it randomly selects a particle from the sort combinations as the generated one for feeding to the adaptive multi-point mutation operator. Fig. 4(a) depicts the neighborhood mutation operator. It randomly chooses the locations  $l_1$ ,  $l_2$  and  $l_3$ , and generates

all sort combinations for the task order. It then randomly selects the second combination as the one for the adaptive multi-point mutation operator.

The adaptive multi-point mutation operator randomly chooses  $k$  locations (*i.e.*, number of mutations) in a particle, and mutates each location's number of servers in the interval  $[1, |\mathbf{S}|]$ . Fig. 4(b) depicts this adaptive multi-point mutation operator. It randomly chooses 3 locations (*i.e.*,  $l_1, l_2$  and  $l_3$ ), and mutates the corresponding number of servers from (2,4,2) to (1,3,4).

For *individual cognition* and *social cognition* parts, we introduce the crossover operator of GA to update the corresponding part of Eq. (24). The updating process is determined by Eqs. (32) and (33).

$$B_i^{t+1} = op^{cr}(A_i^{t+1}, pB_i^t, c_1, r_1) = \begin{cases} C_r(A_i^{t+1}, pB_i^t), r_1 < c_1; \\ A_i^{t+1}, \text{ otherwise.} \end{cases} \quad (32)$$

$$P_i^{t+1} = op^{cr}(B_i^{t+1}, gB^t, c_2, r_2) = \begin{cases} C_r(B_i^{t+1}, gB^t), r_2 < c_2; \\ B_i^{t+1}, \text{ otherwise.} \end{cases} \quad (33)$$

Where  $C_r(\cdot)$  is the two-point crossover operator.  $C_r(A, B)$  randomly selects two locations in the particle A, and then replaces the corresponding segments between the two locations of A with the same interval in the particle B. Fig. 5 depicts this crossover operator in action. It randomly selects the locations  $l_1$  and  $l_2$  in a mutated particle, and replaces the segments between  $l_1$  and  $l_2$  with the same interval in  $pB_i^t$  (or  $gB^t$ ).

Mutated particle	2.3	2	0.9	1	0.7	3	1.2	4	3.9	2	1.5	4	2.3	3	1.5	2
$pB_i^t(gB^t)$	1.9	3	0.3	1	3.1	2	1.7	1	0.7	4	2.5	3	2.3	0	0.1	3
New particle	2.3	2	0.3	1	3.1	2	1.7	1	0.7	4	1.5	4	2.3	3	1.5	2

Fig. 5. Crossover operator.

4) *Mapping from a particle to a fuzzy scheduling*: The mapping from a particle to a fuzzy scheduling in uncertain edge-cloud environments is summarized in Algorithm 1. The inputs are the workflow  $\mathbf{W}$ , all available servers  $\mathbf{S}$ , and an encoded particle  $P$ . The output is the corresponding fuzzy workflow scheduling  $\Psi = (\mathbf{W}, \mathbf{S}, \mathbf{M}, \tilde{t}_t, \tilde{c}_t)$  based on the particle  $P$ . It first initializes the mapping  $\mathbf{M}$  to an empty set *null* and  $\tilde{c}_{tran}$  to (0,0,0). The fuzzy task processing time  $\tilde{t}_{com}(|\mathbf{V}| \times |\mathbf{S}|)$  on different servers, and the fuzzy data transferring time  $\tilde{t}_{tran}(|\mathbf{E}|, |\mathbf{S}| \times |\mathbf{S}|)$  between servers are calculated (line 3). According to the encoded particle  $P$ , each task  $v_i$  is scheduled on the server  $s_j$  with the order  $\chi_j$ . For a certain task  $v_i$ , its start time  $\tilde{t}_{start}(v_i)$  is equal to the booting time  $\zeta_j$  of the server  $s_j$  if it is an entry task. Otherwise, the task cannot start until the last dataset is transferred to  $s_j$  from its parents (line 13-22). Then, the end time  $\tilde{t}_{end}(v_i)$  of  $v_i$  is the sum of its start time  $\tilde{t}_{start}(v_i)$  and its processing time  $\tilde{t}_{com}(v_i, s_j)$  on the server  $s_j$  (line 24). According to Eqs. (6) and (7),  $\tilde{t}_t$  and  $\tilde{c}_t$  are subsequently calculated. Note that if the fuzzy completion time  $\tilde{t}_t$  exceeds the corresponding

**ALGORITHM 1:** Mapping from a particle  $P$  to a fuzzy scheduling strategy  $\Psi$ .

---

**Input:**  $\mathbf{W}, \mathbf{S}, P$ .  
**Output:**  $\Psi = (\mathbf{W}, \mathbf{S}, \mathbf{M}, \tilde{t}_t, \tilde{c}_t)$

- 1 **Initialization** :  $\mathbf{M} \leftarrow null, \tilde{c}_{tran} \leftarrow (0, 0, 0)$ .
- 2 **begin**
- 3 Calculate  $\tilde{t}_{com}(|\mathbf{V}| \times |\mathbf{S}|), \tilde{t}_{tran}(|\mathbf{E}|, |\mathbf{S}| \times |\mathbf{S}|)$ ;
- 4 **for**  $i=1$  to  $i=|\mathbf{V}|$  **do**
- 5  $\mathbf{M} = \mathbf{M} \cup (v_i, s_j)$ ;
- 6 **if**  $v_i$  is a entry task **then**
- 7 **if**  $s_j$  is off **then**
- 8 Turn on  $s_j, \tilde{\zeta}_j = \tilde{\omega}_j = (0, 0, 0)$ ;
- 9 **end**
- 10  $\tilde{t}_{start}(v_i) = \tilde{\zeta}_j$ ;
- 11 **else**
- 12  $maxT = (0, 0, 0)$ ;
- 13 **foreach** parent  $v_p$  of  $v_i$  **do**
- 14  $maxT = maxT \vee ( \tilde{t}_{end}(v_p) + \tilde{t}_{tran}(d_{p,i}, s_q, s_j) )$ ;  
 $// (v_p, s_q), (v_i, s_j) \in \mathbf{M}$ .
- 15  $\tilde{c}_{tran} += fuzzy(c_{q,j}^{tran} \cdot d_{p,i})$ ;  
 $// fuzzy(*)$  is the fuzzification function.
- 16 **end**
- 17 **if**  $s_j$  is off **then**
- 18 Turn on  $s_j, \tilde{\zeta}_j = \tilde{\omega}_j = maxT$ ;
- 19 **end**
- 20  $\tilde{t}_{start}(v_i) = maxT \vee \tilde{\omega}_j$ ;
- 21 **end**
- 22  $\tilde{t}_{end}(v_i) = \tilde{t}_{start}(v_i) + \tilde{t}_{com}(v_i, s_j)$ ;
- 23 **end**
- 24 **end**
- 25 Calculate  $\tilde{t}_t, \tilde{c}_t$  based on (6) and (7);
- 26 **if**  $\tilde{t}_t > D(\mathbf{W})$  **then**
- 27 set  $P$  as infeasible;
- 28 **return** False;
- 29 **end**
- 30 **return**  $\Psi = (\mathbf{W}, \mathbf{S}, \mathbf{M}, \tilde{t}_t, \tilde{c}_t)$ ;
- 31 **end**

---

deadline (*i.e.*,  $t^u > D(\mathbf{W})$ ), the algorithm stops immediately and returns a symbolic value of False, meaning that this particle is infeasible (line 27-29). Finally, it returns the fuzzy scheduling strategy  $\Psi = (\mathbf{W}, \mathbf{S}, \mathbf{M}, \tilde{t}_t, \tilde{c}_t)$  if this particle is feasible (line 31).

5) *Parameter settings*: The inertia weight  $w$  influences the convergence and searchability of PSO-based algorithm [43]. A larger inertia weight helps the algorithm jumping out of local optima, improving its global searchability. By contrast, a smaller inertia weight improves the algorithm's local searchability. This study proposes a new adjustment mechanism that can adaptively adjust the value of inertia weight based on the particle's current state, thereby enhancing the algorithm's overall searchability, as shown in Eq. (34).

$$\begin{cases} w = w_{max} - (w_{max} - w_{min}) \times \exp\left(\frac{d(P_i^t)}{d(P_i^t) - 1.01}\right), \\ d(P_i^t) = \frac{div(gB^t, P_i^t)}{|P_i^t|}, \end{cases} \quad (34)$$



where  $w_{max}$  and  $w_{min}$  represent the predefined maximum and minimum values of  $w$ ,  $div(gB^t, P_i^t)$  represents the number of different encoding values between the current particle  $P_i^t$  and the global best particle  $gB^t$ , and  $|P_i^t|$  represents the size of the particle's encoding space. This mechanism can adaptively adjust the algorithm's searchability according to the difference between the global best particle and current particle. When  $div(gB^t, P_i^t)$  is relatively small, it means that the difference between  $gB^t$  and  $P_i^t$  is small. Thus, the particle's local searchability is expected to be enhanced, increasing the algorithm's convergence. Conversely, a bigger value of  $div(gB^t, P_i^t)$  means to increase the magnitude of  $w$ , enhancing the particle's global searchability.

Regarding the adaptive multi-point mutation, the mutation number  $k$  is adaptively adjusted according to the change of the inertia weight  $w$ , and its adjustment strategy is implemented by Eq. (35).

$$k = k_{max} + (k_{max} - k_{min}) \times \frac{w - w_{min}}{w_{max} - w_{min}}, \quad (35)$$

where  $k_{max}$  and  $k_{min}$  are the predefined maximum and minimum values of the mutation number  $k$ . The inertia weight  $w$  has a positive effect on the mutation number  $k$ . When  $w$  is large, the mutation number  $k$  is increased to enhance the mutation ability so that the algorithm's global searchability can be intensified. On the contrary, if  $w$  is small, then  $k$  is decreased and as such, only limited mutation ability is reserved to maintain the diversity of the population.

The acceleration coefficients  $c_1, c_2$  are dynamically adjusted according to [41], where  $c_1^s$  and  $c_2^s$  denote the start values of  $c_1$  and  $c_2$ , and  $c_1^e$  and  $c_2^e$  denote their end values.

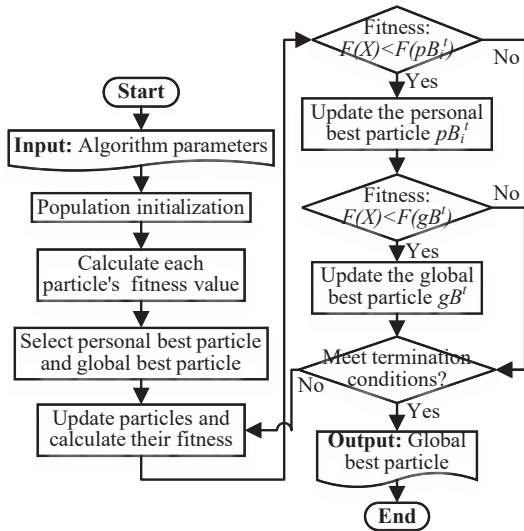


Fig. 6. Flowchart of ADPSO algorithm.

6) *Algorithm flowcharts*: Fig. 6 presents the flowchart of the ADPSO algorithm, which includes the following steps:

**Step 1:** Initialize the parameters of ADPSO, including the population size  $\Gamma$ , the maximum iteration number  $\Theta$ , inertia weight, and acceleration coefficients. Next, randomly generate the initial population.

**Step 2:** Calculate each particle's fitness value according to Eqs. (27-29). Each particle is set to its personal best particle and the particle with the smallest fitness value is set to the global best particle.

**Step 3:** Update all particles according to Eq. (30), and recalculate the fitness value of each updated particle.

**Step 4:** Set the updated particle as the current personal best particle if its fitness value is less than the existing personal best; else, go to **Step 6**.

**Step 5:** Set the updated particle as the global best particle if its fitness value is less than the existing global best.

**Step 6:** Check whether the termination condition is met; if so, output the global best particle and terminate, else, go back to **Step 3**.

## V. PERFORMANCE ANALYSIS

To validate the effectiveness of the workflow scheduling strategy based on the proposed ADPSO, experimental evaluations are carried out. In particular, the following Research Questions (RQs) are checked with the experiments conducted:

**RQ1:** Compared with traditional PSO-based Algorithms, does ADPSO improve the searchability and convergence? (Section V-B)

**RQ2:** In optimizing the fuzzy workflow execution cost, is ADPSO superior to other algorithms in terms of performance stability? (Section V-C)

**RQ3:** In workflow scheduling with respect to given deadlines in uncertain edge-cloud environments, does ADPSO help reduce workflow execution cost? (Section V-D)

### A. Basic experimental setup

All experiments are run on the Win10 64-bit operating system with an Intel(R) Core(TM) i5-7200U CPU at 3.60 GHz and 16 GB RAM. Both ADPSO and all compared algorithms are implemented in Python 3.7. Parameters are set according to [41], where  $\Gamma = 100$ ,  $\Theta = 1000$ ,  $w_{max} = 0.9$ ,  $w_{min} = 0.4$ ,  $k_{max} = |\mathbf{V}|/10$ ,  $k_{min} = 1$ ,  $c_1^s = 0.9$ ,  $c_1^e = 0.2$ ,  $c_2^s = 0.4$ , and  $c_2^e = 0.9$ .

Five types of workflows are tested for this study, obtained from different scientific fields [44], including: CyberShake from earthquake science, Epigenomics from biogenetics, LIGO from gravitational physics, Montage from astronomy, and SIPHT from bioinformatics. Each type of workflow has different structures, numbers of tasks, and data transmissions between tasks, with detailed information stored in an XML file [45]. For each type of workflow, we choose three categories for the experiments: Tiny (approximately 30 tasks), Small (approximately 50 tasks) and Medium (approximately 100 tasks).

There are three cloud servers ( $s_1, s_2, s_3$ ) and two edge servers ( $s_4, s_5$ ) in edge-could environments. Each server has specific processing ability and computation cost per time unit. We assume that  $s_3$  has the most powerful processing ability, the processing time of the tasks on  $s_3$  can be directly recorded from the corresponding XML file. Also, the processing capacity of  $s_1$  or  $s_2$  is approximately half or a quarter of that of  $s_3$ , while the processing capacity of  $s_4$  or  $s_5$  is about one-eighth

or one-tenth of that of  $s_3$ . The computation cost per hour for  $s_3$  is set to  $15.5 \$ \cdot h^{-1}$ , and the other servers' computation cost is approximately proportional to their processing abilities.

The bandwidth and data transmission cost between different types of servers are set as Table I. Each workflow  $\mathbf{W}$  is assumed to have a corresponding deadline constraint in order to test the algorithm performance, set as Eq. (36).

$$D(\mathbf{W}) = 1.5 \times H(\mathbf{W}), \quad (36)$$

where  $H(\mathbf{W})$  represents the execution time for scheduling  $\mathbf{W}$  based on the HEFT algorithm [46].

Section III-C has elaborated how to fuzzify the task processing time  $t_{com}$  and data transferring time  $t_{tran}$  to TFNs. The parameters  $\delta_1$  and  $\delta_2$  are empirically set to 0.85 and 1.2, respectively. For comparing the results effectively among different algorithms, conventional defuzzification method for TFNs [32] is applied to the fuzzy execution cost and fuzzy completion time, where  $\eta$  is set to 1.

### B. RQ1. Searchability and convergence

1) *Compared algorithms*: In this subsection, we regard the traditional PSO [38] as the baseline algorithm for comparison, which adopts a similar order-server nesting encoding strategy. The server encoding value is computed continuously, and its rounding value is set as the server number. The update strategy of PSO is based on Eqs. (24) and (25), and the parameters  $w, c_1, c_2$  are set according to [41]. By comparing the fuzzy execution cost of the candidate solutions and checking the deadline constraint's satisfaction for both algorithms, we analyze their performances in terms of the searchability and convergence.

2) *Results and analysis*: Different time units  $\lambda_i$  are used depending on the size of the workflow. For the tiny and small workflows, the time unit  $\lambda_i$  is one minute. For the medium workflow, the time unit  $\lambda_i$  is one hour. We record both defuzzified fuzzy execution cost and fuzzy completion time of ADPSO and PSO algorithms over 1000 iterations. To clearly illustrate the convergence of fuzzy execution cost and to check whether fuzzy completion time meets the corresponding deadline constraint, Fig. 7 shows the time-cost iteration curves created by ADPSO and PSO algorithms for five types of medium workflow, where a blue full-line, a red dotted-line, and a horizontal black dotted-line indicate the workflow's execution cost, the completion time, and the corresponding deadline, respectively.

ADPSO and PSO algorithms focus on decreasing the workflow completion time during the early global searching, so that they could meet the deadline constraint and obtain a feasible solution. With the increasing of the iteration number, they become emphasizing on optimizing the execution cost within the given deadline while the local search becomes more accurate. The number of iterations required for ADPSO and that for PSO to obtain the first feasible solution are similar. In particular, for CyberShake, as the execution cost is continuously optimizing, the completion time gradually stabilizes, fluctuating within the deadline. However, the scheduling strategy based on PSO becomes stable and converges to the

global optimal particle at around the 200<sup>th</sup> iteration, whilst ADPSO can still update the global optimal particle even at the 700<sup>th</sup> iteration. In terms of the workflow execution cost, the scheduling strategy based on ADPSO is superior to that based on PSO. Regarding LIGO, as the execution cost decreases, the workflow completion time overall tends to decrease as well. Interestingly, the iteration number for convergence by PSO is less than that by ADPSO, but the convergence is reached prematurely as its performance on the execution cost is higher than that of ADPSO. For Montage, from the perspective of fluctuation on the workflow completion time, although PSO may generate the global optimal particle at a latter stage, it has an inapparent improvement concerning the workflow execution cost.

### C. RQ2. Stability on fuzzy execution cost

1) *Compared algorithms*: Apart from the PSO algorithm introduced in Section V-B1, this subsection also describe the following two compared algorithms. (i) Genetic Algorithm (GA) [42]: It employs the same order-server nesting encoding strategy as ADPSO. Following the classical update strategy of GA, the population is updated through binary tournament selection, two-point crossover operator, and mutation operator. Also, this algorithm takes the elitist preservation mechanism and completely copies the elite individuals into the next generation. The crossover probability and mutation probability of GA are set to 0.8 and 0.1, respectively [42]. (ii) Random Searching (RS) [36]: RS also employs the same order-server nesting encoding strategy as ADPSO. The random searching strategy is adopted to generate the new population, with the order and server encoding of each particle being randomly created. In addition, there is no interference between iterations. The optimal solution in the population is produced at the end iteration.

2) *Stability performance index*: To test the stability of all algorithms, the sample variance vector  $\mathbf{var}$  [47] is introduced to measure the performance of each algorithm. The sample variance  $var_i$  of an algorithm is defined by Eq. (37).

$$var_i = \frac{\sum_{j=1}^h (F_j - \bar{F})^2}{h - 1}, \quad (37)$$

where  $i = 1, \dots, 4$  corresponds to the four algorithms: ADPSO, PSO, GA, and RS.  $h$  denotes the number of tests,  $F_j$  denotes the fitness value at the  $j^{\text{th}}$  test, and  $\bar{F}$  denotes the mean fitness value after  $h$  tests.

Due to the uncertainty of fuzzy workflow scheduling, the weak fluctuation can have a significant impact on the fuzzy execution cost. Hence, we consider the relative magnitudes of the variances among the four algorithms and normalize the sample variance vector  $\mathbf{var}$  as follows:

$$\mathbf{var}' = \frac{\mathbf{var}}{\|\mathbf{var}\|_2}, \quad (38)$$

where  $\mathbf{var}'$  is the standardized sample variance vector, and  $\|\cdot\|_2$  is the 2-norm. In general, the smaller the normalized sample variance is, the better stability the algorithm has.

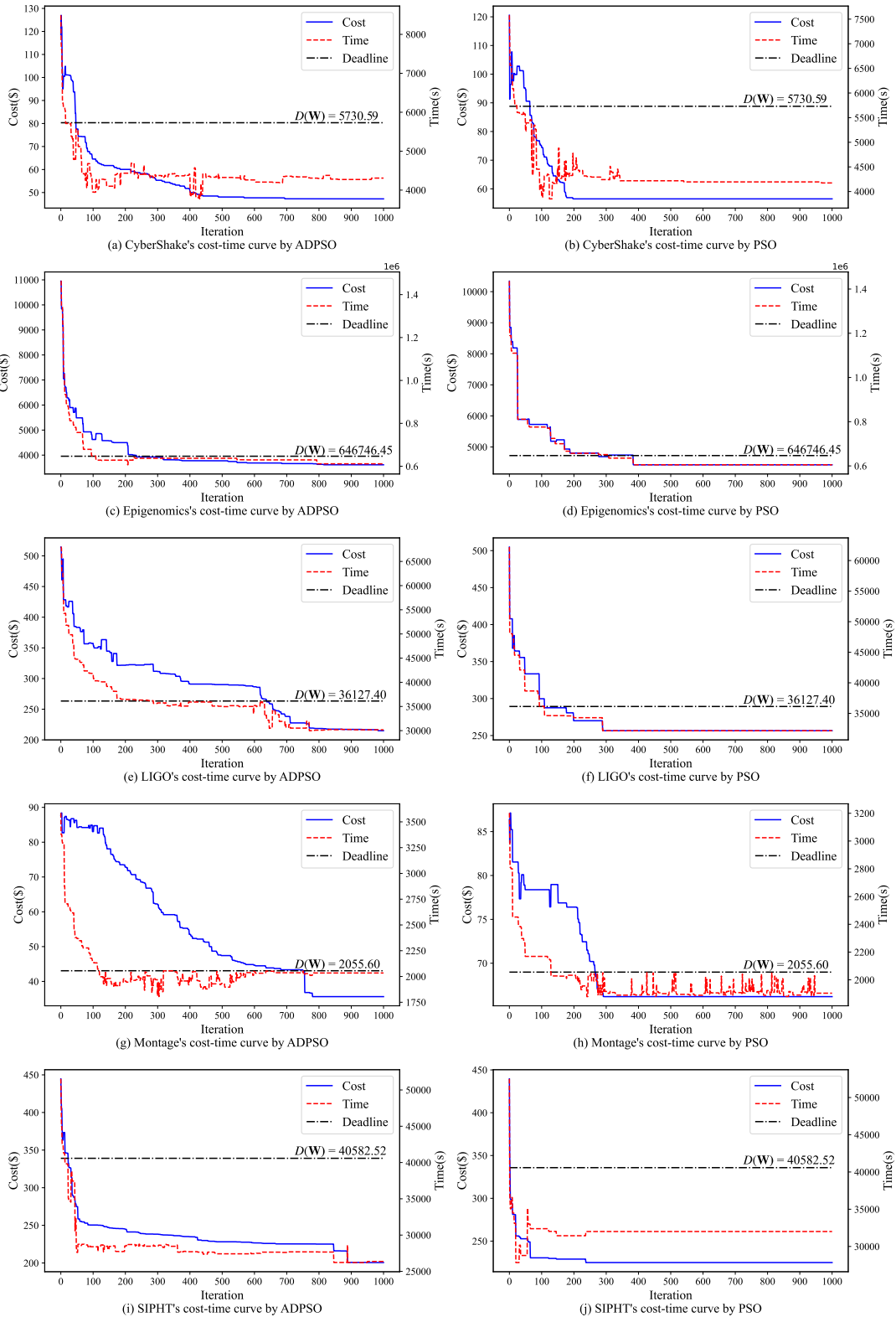


Fig. 7. Time-cost iteration curves created by ADPSO and PSO for five types of medium workflow.

3) *Results and analysis*: For each algorithm, ten independent repeated experiments are carried out, *i.e.*,  $h = 10$ . Table IV shows the normalized sample variances of the fuzzy execution cost for different types of workflow. To visually

compare the normalized sample variances for each workflow among different algorithms, we annotate the minimum and maximum values of the normalized sample variances with the bold and underline fonts, respectively.

As shown in Table IV, ADPSO frequently obtains the

TABLE IV  
NORMALIZED SAMPLE VARIANCES OF FUZZY EXECUTION COST FOR  
DIFFERENT TYPES OF WORKFLOW

Size	Workflows	Algorithms			
		ADPSO	PSO	GA	RS
Tiny	CyberShake	<u>0.67</u>	<b>0.35</b>	0.42	0.49
	Epigenomics	0.61	<u>0.64</u>	<b>0.1</b>	0.45
	LIGO	<b>0.07</b>	0.1	0.08	<u>0.99</u>
	Montage	<b>0.04</b>	0.4	0.38	<u>0.83</u>
	SIPHT	<b>0.02</b>	0.1	<u>0.97</u>	0.23
Small	CyberShake	0.57	<b>0.35</b>	<u>0.58</u>	0.47
	Epigenomics	<b>0.03</b>	0.14	0.04	<u>0.99</u>
	LIGO	<b>0.04</b>	0.09	<u>0.91</u>	0.41
	Montage	<b>0.03</b>	<u>0.84</u>	0.11	0.53
	SIPHT	<b>0.19</b>	0.25	<u>0.89</u>	0.33
Medium	CyberShake	0.5	0.58	<b>0.17</b>	<u>0.62</u>
	Epigenomics	<b>0.02</b>	0.06	0.27	<u>0.96</u>
	LIGO	<b>0.02</b>	<b>0.02</b>	<u>0.87</u>	0.49
	Montage	<b>0.08</b>	0.62	<u>0.77</u>	0.14
	SIPHT	0.35	<b>0.16</b>	0.53	<u>0.76</u>

minimum normalized sample variances, followed by PSO. By contrast, GA and RS frequently obtain the maximum normalized sample variances, while ADPSO has the maximum normalized sample variance only for the case of tiny CyberShake. Furthermore, among these compared algorithms, ADPSO has the smallest normalized sample variance of the fuzzy execution cost among 12 types of workflow. For the case involving tiny workflow, ADPSO obtains the smallest normalized sample variances on 3 workflows. Considering the cases involving small or medium workflows, ADPSO obtains the smallest normalized sample variances over four workflows. In summary, ADPSO has the optimal normalized sample variances, which means that it has the best stability compared with other classical algorithms.

#### D. RQ3. Fuzzy workflow execution cost

1) *Compared algorithms*: The experiments conducted in this subsection also employ those compared algorithms adopted in Section V-C1.

2) *Results and analysis*: To compare the performances of these different algorithms for fuzzy workflow execution cost in the given uncertain edge-cloud environments, we carry out 10 sets of independent repeated experiments for each algorithm with respect to cases involving different types of workflows. For each algorithm with one type of workflow, we record the optimal execution cost and its corresponding fitness (Unit: \$), as well as the mean execution cost and its corresponding fitness (Unit: \$) in the 10 independent repeated experiments.

Table V shows the fuzzy workflow execution cost of different algorithms for the tiny workflows. All the optimal solutions are listed in bold, and all the infeasible solutions are noted by ‘\*’. Except for the case of SIPHT, ADPSO always obtains the optimal solution, beating PSO, GA and RS (with RS having the worst performance, and returning infeasible solutions). The superior performance of ADPSO is mainly owing to the

improved encoding strategy, and the particle update mechanisms adopting the crossover operator and mutation operator of GA. Thus, better scheduling strategy is attained by ADPSO while avoiding premature convergence to local optima. Note that as the solution space of workflow scheduling is generally exponential, the random search strategy of RS is ineffective. As such, given limited population size and iteration number, it is difficult for RS to find high-quality solutions, even returning infeasible solutions.

For the small workflows, experimental results show that the performance of ADPSO is still the best, obtaining all the optimal solutions. For CyberShake, the optimal value of ADPSO is 26.4% better than that of PSO, 15.9% better than that of GA, and 125.5% better than that of RS. In addition, the mean execution cost value of ADPSO beats PSO, GA, and RS by 19.9% for Montage, 16.3% for CyberShake, and 117.6% for Montage, respectively. Indeed, ADPSO outperforms the other algorithms while scheduling CyberShake and Montage which involve the computing-intensive tasks. The scheduling results for medium workflows are almost the same as those for small workflows, with ADPSO achieving optimal solutions for all such workflows. By contrast, RS suffers from the worse performance with the expansion of task sizes, becoming almost impossible to obtain a feasible solution. In short, the scheduling strategy based on ADPSO is able to reduce fuzzy workflow execution cost while achieving better scheduling outcomes compared with other algorithms.

#### E. Engineering Applications



Fig. 8. Vehicle identification application.

Vehicle identification is one of the workflow applications in transportation systems, whose core technology is Deep Neural Networks (DNN) [48], [49]. Traffic cameras with limited process capacity periodically record the images of on-road vehicles, and usually fail to complete the applications within their deadlines. Workflow decision making is one of the key issues to performance DNNs in vehicle identification applications. Fig. 8 presents the outline of the vehicle identification application.

The uncertain environments have a great impact on the system latency for such problems, which can easily lead to the misjudgement of the optimal scheduling. In addition, it is difficult to select an optimal layers-servers solution from the numerous combinations. Therefore, as shown in Fig. 9, we can employ the scheduling strategy based on ADPSO to

TABLE V  
FUZZY WORKFLOW EXECUTION COST OF DIFFERENT ALGORITHMS FOR TINY WORKFLOWS

Workflows	Algorithms	Optimal execution cost and its corresponding fitness (\$)	Mean execution cost and its corresponding fitness (\$)
CyberShake	ADPSO [our]	<b>(8.94,8.98,9.08), 9.02</b>	<b>(11.25,11.48,12.14), 11.74</b>
	PSO [38]	(11.08,11.19,11.60), 11.36	(13.42,13.73,14.66), 14.09
	GA [42]	(9.86,9.93,10.22), 10.05	(12.18,12.49,13.31), 12.81
	RS [42]	(17.96,18.66,20.65), 19.43	(21.07,21.96,24.42), 22.91
Epigenomics	ADPSO	<b>(146.64,154.25,174.53), 162.05</b>	<b>(151.50,159.47,181.36), 167.92</b>
	PSO	(150.71,157.72,173.19), 163.51	(157.01,164.49,177.16), 169.03
	GA	(162.41,166.14,177.28), 170.49	(165.85,171.71,181.42), 175.17
	RS	(168.93,174.57,186.42), 178.98	(173.47,180.76,198.27), 187.40
LIGO	ADPSO	<b>(63.14,64.08,66.81), 65.14</b>	<b>(63.77,65.81,70.11), 67.41</b>
	PSO	(64.80,67.05,72.19), 68.98	(67.28,69.06,73.61), 70.80
	GA	(64.59,66.27,70.48), 67.88	(66.90,68.27,72.09), 69.75
	RS	(79.77,81.74,86.06), 83.36*	(87.39,89.05,93.78), 90.88
Montage	ADPSO	<b>(3.89,3.99,4.17), 4.05</b>	<b>(4.11,4.24,4.48), 4.32</b>
	PSO	(4.79,4.92,5.33), 5.08	(5.44,5.64,6.16), 5.84
	GA	(4.79,5.00,5.32), 5.11	(5.52,5.76,6.30), 5.96
	RS	(12.45,13.07,14.53), 13.62	(13.76,14.49,16.28), 15.17
SIPHT	ADPSO	(56.26,58.05,64.33), 60.54	<b>(56.58,58.38,64.79), 60.93</b>
	PSO	<b>(58.51,59.79, 61.88), 60.53</b>	(59.41,60.90,63.78), 61.95
	GA	(60.69,60.84,61.31), 61.02	(62.21,63.41,65.96), 64.36
	RS	(68.62,69.60,72.03), 70.52	(70.62,71.72,74.62), 72.84

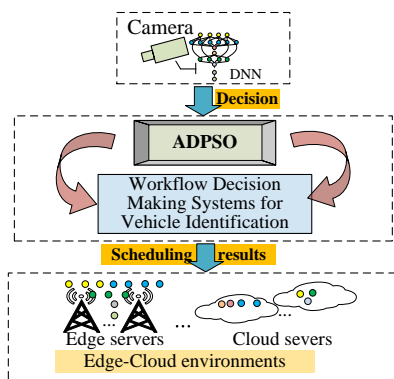


Fig. 9. Scheduling strategy based on ADPSO for vehicle identification in uncertain edge-cloud environments.

make intelligent workflow decisions for vehicle identification applications, which can reduce the execution cost mainly caused by layer computation and data transmission between layers within their deadlines, even in uncertain edge-cloud environments. Complex DNN layers (tasks) in vehicle identification applications can be scheduled to the cloud for execution, while simple ones are processed on the edge. The cloud and edge platforms collaborate with each other and execute the DNN layers with low system cost and latency.

## VI. CONCLUSION AND THE FUTURE WORK

This paper has proposed a cost-driven scheduling strategy based on ADPSO for deadline-based workflow applications in uncertain edge-cloud environments. The work enables the reduction of workflow execution cost that is mainly caused by task computation and data transmission, while satisfying given deadlines. Experimental results have shown that the proposed

strategy offers a better performance on scheduling computing-intensive workflows than the state-of-the-art approaches. Particularly, ADPSO can obtain the optimal fuzzy execution cost for almost all types of workflows investigated.

Our future work intends to improve the current strategy to address more types of workflow applications (than experimentally studied herein), as well as workflow ensembles in fuzzy edge-cloud environments. Also, to reflect the fact that in general, different tasks may have different requirements, we plan to refine the proposed approach to consider different load-to-cost ratios for different servers, while optimizing the overall workflow scheduling process.

## REFERENCES

- [1] W. Fang, F. Xue, Y. Ding, N. Xiong, and V. C. M. Leung, "Edgeke: An on-demand deep learning iot system for cognitive big data on industrial edge devices," *IEEE Transactions on Industrial Informatics*, vol. 17, no. 9, pp. 6144–6152, 2021.
- [2] B. Lin, Y. Huang, J. Zhang, J. Hu, X. Chen, and J. Li, "Cost-driven off-loading for DNN-based applications over cloud, edge, and end devices," *IEEE Transactions on Industrial Informatics*, vol. 16, no. 8, pp. 5456–5466, 2020.
- [3] P. Han, C. Du, J. Chen, F. Ling, and X. Du, "Cost and makespan scheduling of workflows in clouds using list multiobjective optimization technique," *Journal of Systems Architecture*, p. 101837, 2020.
- [4] H. Yuan, J. Bi, W. Tan, M. Zhou, B. H. Li, and J. Li, "TTSA: An effective scheduling approach for delay bounded tasks in hybrid clouds," *IEEE Transactions on Cybernetics*, vol. 47, no. 11, pp. 3658–3668, 2017.
- [5] G. Ismayilov and H. R. Topcuoglu, "Neural network based multi-objective evolutionary algorithm for dynamic workflow scheduling in cloud computing," *Future Generation Computer Systems*, vol. 102, pp. 307–322, 2020.
- [6] S. Meng, W. Huang, X. Yin, M. R. Khosravi, Q. Li, S. Wan, and L. Qi, "Security-aware dynamic scheduling for real-time optimization in cloud-based industrial applications," *IEEE Transactions on Industrial Informatics*, pp. 1–10, 2020.

- [7] W. Shu, K. Cai, and N. N. Xiong, "Research on strong agile response task scheduling optimization enhancement with optimal resource usage in green cloud computing," *Future Generation Computer Systems*, vol. 124, pp. 12–20, 2021.
- [8] W. Wang, Y. Jiang, and W. Wu, "Multiagent-based resource allocation for energy minimization in cloud computing systems," *IEEE Transactions on Systems, Man, and Cybernetics: Systems*, vol. 47, no. 2, pp. 205–220, 2017.
- [9] B. Lin, F. Zhu, J. Zhang, J. Chen, X. Chen, N. N. Xiong, and J. Lloret Mauri, "A time-driven data placement strategy for a scientific workflow combining edge computing and cloud computing," *IEEE Transactions on Industrial Informatics*, vol. 15, no. 7, pp. 4254–4265, 2019.
- [10] T. Taleb, K. Samdanis, B. Mada, H. Flinck, S. Dutta, and D. Sabella, "On multi-access edge computing: A survey of the emerging 5G network edge cloud architecture and orchestration," *IEEE Communications Surveys & Tutorials*, vol. 19, no. 3, pp. 1657–1681, 2017.
- [11] Q. Luo, S. Hu, C. Li, G. Li, and W. Shi, "Resource scheduling in edge computing: A survey," *IEEE Communications Surveys & Tutorials*, vol. 23, no. 4, pp. 2131–2165, 2021.
- [12] X. Chen, J. Zhang, B. Lin, Z. Chen, K. Wolter, and G. Min, "Energy-efficient offloading for DNN-based smart IoT systems in cloud-edge environments," *IEEE Transactions on Parallel and Distributed Systems*, vol. 33, no. 3, pp. 683–697, 2022.
- [13] Y.-H. Jia, W.-N. Chen, H. Yuan, T. Gu, H. Zhang, Y. Gao, and J. Zhang, "An intelligent cloud workflow scheduling system with time estimation and adaptive ant colony optimization," *IEEE Transactions on Systems, Man, and Cybernetics: Systems*, vol. 51, no. 1, pp. 634–649, 2021.
- [14] Z.-G. Chen, Z.-H. Zhan, Y. Lin, Y.-J. Gong, T.-L. Gu, F. Zhao, H.-Q. Yuan, X. Chen, Q. Li, and J. Zhang, "Multiobjective cloud workflow scheduling: A multiple populations ant colony system approach," *IEEE Transactions on Cybernetics*, vol. 49, no. 8, pp. 2912–2926, 2019.
- [15] Z. Wen, S. Garg, G. S. Aujla, K. Alwasel, D. Puthal, S. Dustdar, A. Y. Zomaya, and R. Ranjan, "Running industrial workflow applications in a software-defined multicloud environment using green energy aware scheduling algorithm," *IEEE Transactions on Industrial Informatics*, vol. 17, no. 8, pp. 5645–5656, 2021.
- [16] L. Sun, L. Lin, M. Gen, and H. Li, "A hybrid cooperative coevolution algorithm for fuzzy flexible job shop scheduling," *IEEE Transactions on Fuzzy Systems*, vol. 27, no. 5, pp. 1008–1022, 2019.
- [17] D. Gao, G. Wang, and W. Pedrycz, "Solving fuzzy job-shop scheduling problem using de algorithm improved by a selection mechanism," *IEEE Transactions on Fuzzy Systems*, vol. 28, no. 12, pp. 3265–3275, 2020.
- [18] P. K. Muhuri, R. Nath, and A. K. Shukla, "Energy efficient task scheduling for real-time embedded systems in a fuzzy uncertain environment," *IEEE Transactions on Fuzzy Systems*, vol. 29, no. 5, pp. 1037–1051, 2021.
- [19] S. Feng and C. L. P. Chen, "A fuzzy restricted boltzmann machine: Novel learning algorithms based on the crisp possibilistic mean value of fuzzy numbers," *IEEE Transactions on Fuzzy Systems*, vol. 26, no. 1, pp. 117–130, 2018.
- [20] J. Sahni and D. P. Vidyarthi, "A cost-effective deadline-constrained dynamic scheduling algorithm for scientific workflows in a cloud environment," *IEEE Transactions on Cloud Computing*, vol. 6, no. 1, pp. 2–18, 2018.
- [21] T. Pham and T. Fahringer, "Evolutionary multi-objective workflow scheduling for volatile resources in the cloud," *IEEE Transactions on Cloud Computing*, pp. 1–12, 2020.
- [22] P. Paknejad, R. Khorsand, and M. Ramezani, "Chaotic improved picea-g-based multi-objective optimization for workflow scheduling in cloud environment," *Future Generation Computer Systems*, vol. 117, pp. 12–28, 2021.
- [23] Y. Jararweh, "Enabling efficient and secure energy cloud using edge computing and 5G," *Journal of Parallel and Distributed Computing*, vol. 145, pp. 42–49, 2020.
- [24] Y. Xie, Y. Zhu, Y. Wang, Y. Cheng, R. Xu, A. S. Sani, D. Yuan, and Y. Yang, "A novel directional and non-local-convergent particle swarm optimization based workflow scheduling in cloud-edge environment," *Future Generation Computer Systems*, vol. 97, pp. 361–378, 2019.
- [25] Q. Peng, H. Jiang, M. Chen, J. Liang, and Y. Xia, "Reliability-aware and deadline-constrained workflow scheduling in mobile edge computing," in *2019 IEEE 16th International Conference on Networking, Sensing and Control (ICNSC)*, 2019, pp. 236–241.
- [26] A. H. Gandomi and A. H. Alavi, "Krill herd: A new bio-inspired optimization algorithm," *Communications in Nonlinear Science and Numerical Simulation*, vol. 17, no. 12, pp. 4831–4845, 2012.
- [27] D. Lei, "Fuzzy job shop scheduling problem with availability constraints," *Computers & Industrial Engineering*, vol. 58, no. 4, pp. 610–617, 2010.
- [28] P. Fortemps, "Jobshop scheduling with imprecise durations: a fuzzy approach," *IEEE Transactions on Fuzzy Systems*, vol. 5, no. 4, pp. 557–569, 1997.
- [29] K. Li, J. Chen, H. Fu, Z. Jia, and W. Fu, "Uniform parallel machine scheduling with fuzzy processing times under resource consumption constraint," *Applied Soft Computing*, vol. 82, p. 105585, 2019.
- [30] Y. Yin, T. C. E. Cheng, D. Wang, and C.-C. Wu, "Improved algorithms for single-machine serial-batch scheduling with rejection to minimize total completion time and total rejection cost," *IEEE Transactions on Systems, Man, and Cybernetics: Systems*, vol. 46, no. 11, pp. 1578–1588, 2016.
- [31] Q. Shen and R. Leitch, "Fuzzy qualitative simulation," *IEEE Transactions on Systems, Man, and Cybernetics*, vol. 23, no. 4, pp. 1038–1061, 1993.
- [32] L. A. Zadeh, "The concept of linguistic variable and its application to approximate reasoning," *Information Sciences*, vol. 8, no. 3, pp. 199–249, 1975.
- [33] E. Lee and R.-J. Li, "Comparison of fuzzy numbers based on the probability measure of fuzzy events," *Computers & Mathematics with Applications*, vol. 15, no. 10, pp. 887–896, 1988.
- [34] J. J. Palacios, M. A. González, C. R. Vela, I. González-Rodríguez, and J. Puente, "Genetic tabu search for the fuzzy flexible job shop problem," *Computers & Operations Research*, vol. 54, pp. 74–89, 2015.
- [35] M. Sakawa and R. Kubota, "Fuzzy programming for multi-objective job shop scheduling with fuzzy processing time and fuzzy due date through genetic algorithms," *European Journal of Operational Research*, vol. 120, no. 2, pp. 393–407, 2000.
- [36] B. Zhou, S. Xie, F. Wang, and J. Hui, "Multi-step predictive compensated intelligent control for aero-engine wireless networked system with random scheduling," *Journal of the Franklin Institute*, vol. 357, no. 10, pp. 6154–6174, 2020.
- [37] M. H. Shirvani, "A hybrid meta-heuristic algorithm for scientific workflow scheduling in heterogeneous distributed computing systems," *Engineering Applications of Artificial Intelligence*, vol. 90, p. 103501, 2020.
- [38] J. Kennedy and R. Eberhart, "Particle swarm optimization," in *Proceedings of ICNN'95 - International Conference on Neural Networks*, vol. 4, 1995, pp. 1942–1948.
- [39] W. Guo, J. Li, G. Chen, Y. Niu, and C. Chen, "A PSO-optimized real-time fault-tolerant task allocation algorithm in wireless sensor networks," *IEEE Transactions on Parallel and Distributed Systems*, vol. 26, no. 12, pp. 3236–3249, 2015.
- [40] M. A. Rodriguez and R. Buyya, "Deadline based resource provisioning and scheduling algorithm for scientific workflows on clouds," *IEEE Transactions on Cloud Computing*, vol. 2, no. 2, pp. 222–235, 2014.
- [41] Y. Shi and R. Eberhart, "A modified particle swarm optimizer," in *1998 IEEE International Conference on Evolutionary Computation Proceedings. IEEE World Congress on Computational Intelligence (Cat. No.98TH8360)*, 1998, pp. 69–73.
- [42] L. Cui, J. Zhang, L. Yue, Y. Shi, H. Li, and D. Yuan, "A genetic algorithm based data replica placement strategy for scientific applications in clouds," *IEEE Transactions on Services Computing*, vol. 11, no. 4, pp. 727–739, 2018.
- [43] X.-F. Song, Y. Zhang, D.-W. Gong, and X.-Z. Gao, "A fast hybrid feature selection based on correlation-guided clustering and particle swarm optimization for high-dimensional data," *IEEE Transactions on Cybernetics*, pp. 1–14, 2021.
- [44] S. Bharathi, A. Chervenak, E. Deelman, G. Mehta, M. Su, and K. Vahi, "Characterization of scientific workflows," in *2008 Third Workshop on Workflows in Support of Large-Scale Science*, 2008, pp. 1–10.
- [45] R. F. D. Silva, "Workflowhub," [EB/OL], 2020, <https://confluence.pegasus.isi.edu/display/pegasus/WorkflowHub>.
- [46] H. Topcuoglu, S. Hariri, and Min-You Wu, "Performance-effective and low-complexity task scheduling for heterogeneous computing," *IEEE Transactions on Parallel and Distributed Systems*, vol. 13, no. 3, pp. 260–274, 2002.
- [47] A.-M. Tyrisev, W. Fikse, E. Mntysaari, J. Jakobsen, G. Aamand, J. Dürr, and M. Lidauer, "Validation of consistency of mendelian sampling variance," *Journal of Dairy Science*, vol. 101, no. 3, pp. 2187–2198, 2018.
- [48] X. Chen, M. Li, H. Zhong, Y. Ma, and C.-H. Hsu, "DNNOff: Offloading DNN-based intelligent IoT applications in mobile edge computing," *IEEE Transactions on Industrial Informatics*, vol. 18, no. 4, pp. 2820–2829, 2022.

- [49] M. Liu, W. Fang, X. Ma, W. Xu, N. Xiong, and Y. Ding, "Channel pruning guided by spatial and channel attention for dnns in intelligent edge computing," *Applied Soft Computing*, vol. 110, p. 107636, 2021.



Management.

**Bing Lin** is currently an associate professor with the College of Physics and Energy at Fujian Normal University. Now he is a visiting scholar at School of Computer Science, Peking University. His research interest mainly includes parallel and distributed computing, computational intelligence, and data center resource management. He has published over thirty journals and conference articles, such as IEEE Transactions on Parallel and Distributed Systems, IEEE Transactions on Industrial Informatics, and IEEE Transactions on Network and Service



**Chaowei Lin** received the B.S. degree in Information and Computing Science from Fuzhou University, Fujian, China, in 2020. He is currently a postgraduate in Computer Software and Theory at the College of Mathematics and Computer Science, Fuzhou University, Fujian, China. His current research interests include workflow scheduling, computational intelligence, edge computing, and cloud computing.



**Xing Chen** is a Professor at Fuzhou University, and the Director of Fujian Key Laboratory of Network Computing and Intelligent Information Processing. He received the B.S. degree and the Ph.D. degree from Peking University, in 2008 and 2013, respectively. He joined Fuzhou University since 2013. He focuses on the software systems and engineering approaches for cloud and mobility. His current projects cover the topics from self-adaptive software, computation offloading, model driven approach and so on. He has published over 80 journal and conference articles, including IEEE Transactions on Parallel and Distributed Systems, IEEE Transactions on Cloud Computing, IEEE Transactions on Industrial Informatics, etc.